International Journal of Research in Advent Technology, Vol.7, No.5, May 2019
E-ISSN: 2321-9637
Available online at www.ijrat.org

Photocatalytic degradation of Rhodamine B using SiO_2 supported on activated carbon

S.K Nirmala[1], P.Rajesh[1*], R. Venckatesh[2], Rajeswari sivaraj[2] and M. Ezhil Inban[3]
[1]*Department of Chemistry, Government Arts College, Coimbatore - 641018, Tamil Nadu, India*
[2]*Department of Chemistry, Government Arts College, Udumalpet - 642126, TamilNadu, India*
[3]*Department of Physics, Government Arts College, Coimbatore- 641 018, Tamil Nadu, India*
Email : nirmala.sathy2010@gmail.com[1], gacchemistryrajesh@gmail.com[2], rvenckat@gmail.com[3], rajeshwarishivaraj@gmail.com[4]

Abstract-SiO_2 sol was prepared by using Silicic acid with Tetrahydrofuran in the ratio of 1:2 along with Isopropanol solution and mixed with *Coccinia indica* bark activated carbon (AC) prepared using acid impregnation method. The grain size of the particles was calculated by X-ray diffraction, SEM and EDAX analysis reported the surface morphology and chemical composition. The crystal structure and elemental composition was analyzed by Fourier transform spectroscopy, band gap was calculated using UV–Visible spectroscopy. The photocatalytic experiments were performed with aqueous solution of Rhodamine B for 2h irradiation, direct photolysis of AC–SiO_2 contributed 85% decomposition in solar radiation for the optimized concentration of Rhodamine B dye.

Keywords: Photocatalysis, Silica, Activated carbon, Nanocomposite, Rhodamine B

1. INTRODUCTION

The development of better catalysts for water treatment is a significant contribution of Nano science. Among the advanced oxidation processes, photocatalysis-using semiconductors has become a leading technology in the field of environmental cleaning. Silica is suitable in many areas like ceramics, glass industries, photovoltaic cells [1, 2]. SiO_2 exhibits measurable activities for catalytic and photocatalytic reactions [3, 4]. Bi-metal and tri-metal doped SiO_2 has become of interest in promoting photocatalytic reactions under UV- light irradiation [5, 6]. Now-a-days, the sol-gel technique is the most commonly employed for the synthesis of silica as well as metal doped SiO_2 core-shell matrices [7]. It involves simultaneous hydrolysis and condensation of alkoxides, so that silica with several characteristics can be produced [8, 9]. Various supported materials have been proposed for degradation of several dye molecules [10-12]. Activated carbon (AC) is excellent adsorbent of countless pollutants. It is very promising as it is able to adsorb the dye molecules and then release them onto the surface of the catalysts. The intermediates produced during degradation can be adsorbed by AC and then oxidized [13, 14]. Their industrial applications involve the adsorptive removal of odour, colour, taste and other undesirable organics from industrial wastewater [15].In the present paper, the possibility of utilization of the AC-SiO_2 nanocomposite for the photocatalytic removal of Rhodamine B dye from an aqueous medium has been investigated. The equilibrium study has been observed to study the effects of various process parameters such as P_H, contact time and sorbent dosage on the photocatalytic process. Equilibrium data have been fit into various adsorption isotherms in order to select an appropriate isotherm model.

2. EXPERIMENTAL DETAILS

2.1. Biomass preparation

Coccinia indica bark was washed with tap water, then rinsed with double-de-ionized water and dried first in the sun light for 7 days. Resulting dried bark was cut into small pieces and used for further studies.

2.2. Impregnation using sulfuric acid (H_2SO_4)

In a 5L trough 500 g of *Coccinia indica* bark was contacted 500 ml sulphuric acid during a fixed period of impregnation time, temp (16]. The impregnated samples were recovered by filtration and dried at room temperature for 2 days. They were calcined in a muffle furnace for 3 h. Later the activated carbon was rinsed with double-ionized water until pH 6, dried in hot air oven for 4 h, and used for further studies.

2.3. Preparation of carbon - SiO_2 nanocomposite

Silicic acid with Tetrahydrofuran in the ratio of 1:2 was used for the preparation of SiO_2 sol. Isopropanol solution was added to the above mixture with continuous stirring for 2h and irradiated in microwave oven for 30 min. The prepared gel was mixed well with weighed amount of prepared activated carbon with continuous stirring for 1h. The reaction products were filtered, washed with deionized water and dried in hot air oven at 80^oC.

The cationic dye, Rhodamine B was purchased from Sigma-Aldrich. All the above reagents were analytical grade without any additional purification. Deionized water was used throughout the reactions and synthesis process. Besides, all the experimental tests were performed at room temperature.

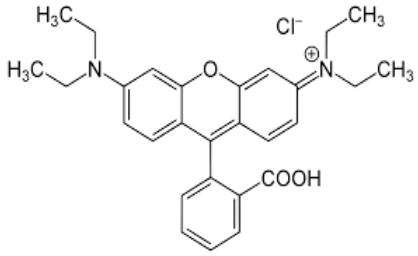

Fig.1. Structure of Rhodamine B (Mol.F $C_{28}H_{31}ClN_2O_3$)

2.4. Characterization

The prepared AC-SiO_2 nanocomposites was characterized for the crystalline structure using D8 Advance X-ray diffraction meter (Bruker AXS, Germany) at room temperature, operating at 30 kV and 30 mA, using Cu$K\alpha$ radiation (λ = 0.15406 nm). The crystal size was calculated by Scherrer's formula. Surface morphology was studied by using SEM-EDS (Model JSM 6390LV, JOEL, USA), UV–Vis diffuse reflectance spectra was recorded with a Carry 5000 UV-Vis-NIR spectrophotometer (Varian, USA) and FTIR spectra were measured on an AVATAR 370-IR spectrometer (Thermo Nicolet, USA) with a wave number range of 4000 to 400 cm^{-1}.

2.5. Photocatalytic activity

The photocatalytic activity of the AC- SiO_2 was studied under solar irradiation. In a typical experiment, aqueous suspensions of Rhodamine B dye solutions (20, 40, 60, 80 mg/L) and 0.1 g of the AC - photo catalysts were placed in reaction bottles. Prior to irradiation, the suspension was stirred magnetically to ensure an adsorption/desorption equilibrium. At regular intervals of given irradiation time the suspension were withdrawn, filtered and measured spectrophotometrically (554 nm). The effect of catalyst load was studied using (50 to 300mg) of the adsorbent and pH study was carried out from 2 -12 for all the four concentrations of the dye.

3. RESULTS AND DISCUSSION

3.1. Characterization of the photocatalyst

The ultraviolet-visible spectrum shows strong absorption bands in the visible spectral region with a maximum at 554 nm. The ultraviolet-visible spectrum of Methylene blue dye shows strong absorption bands in the visible spectral region with a maximum at 662 nm. The SEM images of AC- SiO_2 show that the nanoparticles possess an almost spherical shape with homogenous distribution of Si particles throughout the amorphous carbon. AC- SiO_2 shows an average particle size of 35 - 40 nm [2a]. Additionally, the AC- SiO_2 agglomerates possess a rough and porous surface, resulting in an increased surface area, which suggests that this nanocomposite could be chemically reactive, therefore suitable for photocatalytic applications. EDX analysis confirms the presence of Si, C and O in Ac-SiO_2 with peaks for the elements Si, O and C appearing at 1.7 keV, 0.5 keV and 0.3 keVs,. TEM image of the sample [2b] demonstrates that the sample is entirely amorphous Furthermore, the mesoporous SiO_2 has a three dimensionally interconnected and disordered globular-like mesopore structure and the size of mesopore is almost homogeneous. The FTIR spectrum [2 c] reports absorption peak near 1100 cm^{-1}, which corresponds to the Si–O–Si stretching vibrations. The broad band around 3403 cm^{-1} is attributed to O–H stretching and the peak near 1630 cm^{-1} to O–H bending which is related to physically absorbed moisture. It is considered that the dopant Si enhanced the water absorption and the more OH were formed. Thereby, the photo-catalytic activity of AC - $SiO_2$was increased [17]. The XRD results show broad peak at 2θ = 48.0, 54.0 and 62.0 corresponding to the (200), (211) and (204) crystal planes reflection of anatase. [18, 19], The XRD of the modified sample shows hump at 2 theta range (40-50) deg., this means that the composite is highly disordered and amorphous in nature.

3.2. Photocatalytic studies

3.2.1. Initial dye concentration

Fig. 3a. shows the effect of initial dye concentration on photo degradation by the AC-SiO_2 nanocomposite. The results show that the decomposition of Rhodamine B decreased with increasing initial dye concentrations of the dye from 20 to 80 mg/L .It may be concluded that the disappearance of Rhodamine B molecules may be due to their photocatalysis instead of only due to their adsorption. AC modified nanocomposites with high surface area work well as an effective sorbent to concentrate the molecules around the loaded AC-SiO_2 nanocomposite and then provide high dye concentrations for photocatalytic reactions [20, 21]. However, at high concentration of Rhodamine B, lower adsorption efficiency was reported due to saturation of active sites on the adsorbent's surface [22, 23]. This shows that as

the initial concentration of the dye increases, the requirement of catalyst surface needed for the decomposition also increases. Since irradiation time and amount of catalyst are constant, the –OH radical formed on the surface of AC-SiO_2 is also constant and hence the relative number of free radicals attacking the dye molecules decreases with increasing catalyst load [24].

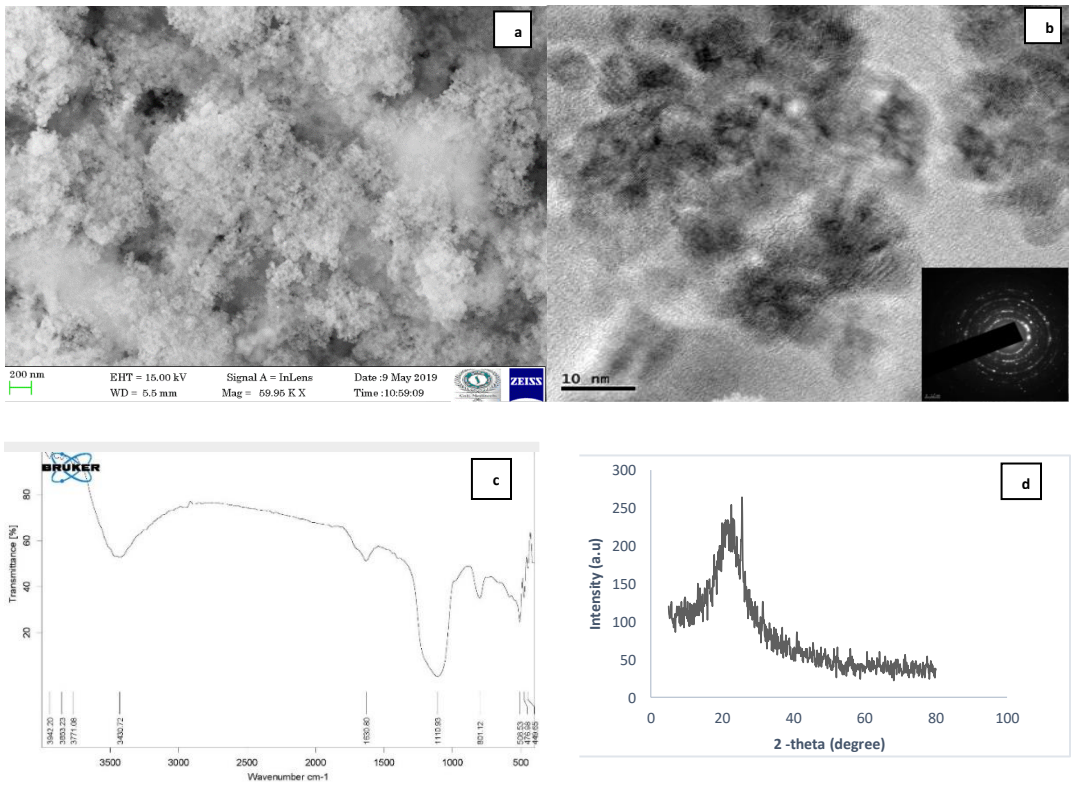

Fig. 2. (a) SEM (b) TEM (c) FTIR (d) XRD image of AC- SiO_2 carbon

3.2.2. Effect of contact time

The photocatalytic percent degradation of Rhodamine against the irradiation time is shown in Fig. 4b. The concentration of Rhodamine B decreases exponentially with the time (2h) for the samples. When time increases more and more light energy falls on the catalyst surfaces which increases the formation of photo excited species and enhances the photocatalytic activity. Moreover the higher surface area and small particle size of the modified catalyst also contribute to the higher activity.

3.2.3. Effect of catalyst amount

Studies report two hour irradiation to a 50 ml aqueous solution of Rhodamine B (20,40,60 and 80 mg/L) with a catalyst of amount from 50m to 300mg. Results show that the percent degradation of the modified catalysts increase with increase in the amount of catalyst and reaches a maximum of 300mg. This shows that the active site provided for the adsorption of substrate on the catalyst surface is limited to catalyst amount of 3g/L. The increase in the degradation efficiency of the dye (95%) with an increase in the catalyst amount may be due to an increase in the active sites available on the catalyst surface for the reaction, which in turn increases the rate of radical formation. With a higher catalyst loading the deactivation of activated molecules by collision with ground state molecules may dominate the reaction, thus reducing the rate of reaction [25].

3.2.4. Effect of pH

Rhodamine B displays a general trend of slightly increased adsorption on Ac-SiO_2 with the increase of solution pH values [Fig.3D.] At pH higher than 2 the adsorption amount of Rhodamine B slightly increased with the increase of solution pH values. In addition, at low pH there was competition for the surface sited of activated carbon between protonation (H^+ adsorption on the carbon surface) and adsorption of Rhodamine B. When pH of solution increases with increasing amount of adsorbed because the increase of solution pH values, the electrical repulsion force

become weaker and the Rhodamine B may be transported to the surface of the Ac-SiO_2 and become attached on the surface due to the action of other factors such as less competition from protonation.

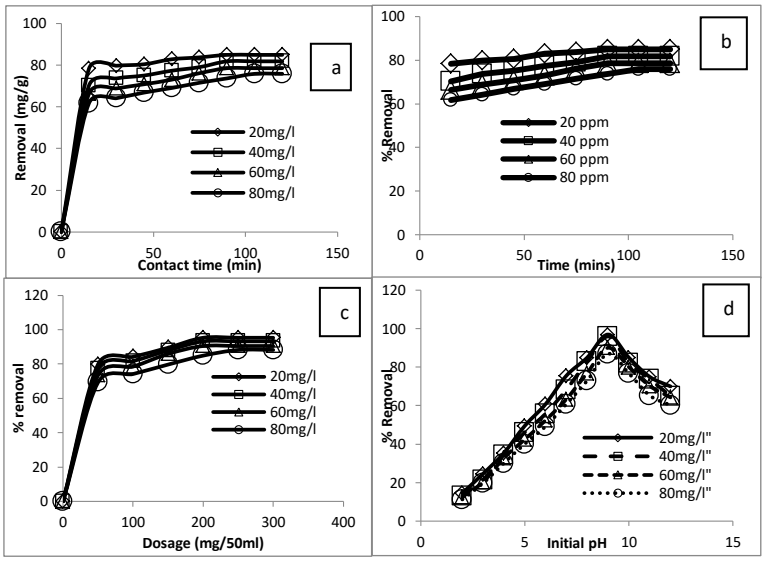

Fig.3. Adsorption and photocatalytic oxidation effects of (a) contact time, (b) concentration (c) dose (d) pH for RB adsorption onto Ac-SiO_2 nanocomposite

3.3. Adsorption Kinetics study

Many attempts have been made to formulate a general expression describing the kinetics of sorption on solid surfaces for liquid– solid phase sorption systems. Lagergren first represented the pseudo-first order equation for the adsorption of oxalic acid and malonic acid onto charcoal. The Lagergren kinetic model has been used to investigate the mechanism of sorption and potential rate controlling steps such as mass transport and chemical reaction processes

3.3.1. Pseudo-first order equation

The pseudo-first order equation of Lagergren is generally expressed as follows:

$$\log(q_e - q_t) = (\log q_e - (K_{ad}/2.303) \times t \quad (1)$$

where q_e is the amount of dye adsorbed (mg/g) at equilibrium; q_t is the amount of dye adsorbed (mg/g) at time, (t), K_{ad} is the rate constant of adsorption, (1/min) and t is agitation time (min.)

Linear plots of log (q_e-qt) Vs t show the applicability of the above model [Fig.4a]. The K_{ad} values have been calculated from the slope of the linear plots and are represented in Table 1 for different concentrations of the dyes studied. The rate constants observed are comparable with the values reported earlier [26]. Diffusive transport through the internal pores of the nanocomposites and/or along the pore–wall surface (intraparticle diffusion) adsorption or attachment of the solute particle at a suitable site on the nanoparticle surface one or more of the above steps may be the rate controlling factor.

3.3.2. Pseudo-second-order model

The pseudo-second-order model is represented by the following differential equation:

$$dq_t/dt = k_2 (q_e - q_t)^2 \quad (2)$$

where q_e = Amount of dye adsorbed (mg/g at equilibrium),q_t = amount of dye adsorbed (mg/g at time t) k^2 is the equilibrium rate constant of pseudo-second order (g/mg/min) adsorption. Integrating the above equation for the boundary condition t = 0 tot and qt = 0 to q, gives:

$$\mathbf{t/q = 1/k_2 q_e^2 + 1/q_e \,.\, t} \quad (3)$$

The slope and intercept of plot of t/q versus t were used to calculate the second-order rate constant k^2 (Fig.4b, Table 1). The correlation coefficients of all examined data were found very high which showed that the model can be applied for the entire adsorption process. From the figure it can be concluded that pseudo-second-order

model was the best fit for the experimental data at different initial Rhodamine B concentrations and suggested that the adsorption of Rhodamine B may be due to electrostatic attraction between the charged surface and charged dyes molecules and may be inclined physisorption to a lesser extent and more towards chemisorption with increase in irradiation time [27].

3.3.3. Adsorption equilibrium study

The experiment equilibrium adsorption data were analyzed using Langmuir and Freundlich adsorption isotherm The adsorption isotherms demonstrate the specific relation between the adsorption capacity of an adsorbent and the concentration of adsorbate at a constant temperature.

3.3.3.1. Langmuir and Freundlich isotherms

Langmuir isotherm can be expressed as

$$q_e = \{(Q_0 \times b \times C_e) / (1 + (b \times C_e)\} \quad (4)$$

where Q_0 is the maximum adsorption capacity per adsorbent mass (mg g-1) and b is a constant related to the adsorption energy (L mg^{-1}). The Freundlich adsorption equation model is expressed by

$$q_e = K_f Ce^{1n} \quad (5)$$

where K_f and 1/n are the Freundlich constants, and K_f represents the relative adsorption capacity of the adsorbent and n represents the adsorption dependence on equilibrium concentration of Rhodamine B. The slopes of the linear form of Langmuir and Freundlich plots [Fig.4c and 4d] were used to determine the adsorption constants tabulated in Table 1. In the present investigation, the value of R_L was less than one which showed that the adsorption process was favorable [28]. The regression coefficients show that the adsorption data has a better fit to Langmuir than to the Freundlich isotherm which may be due to the monolayer coverage of the dye on the Ac-SiO_2 nanocomposite. However, as the process is multistage process the data fit well into both the isotherm models

3.3.3.2. Elovich equation.

The simple Elovich model equation is generally expressed by the following equation

$$q_t = \alpha + \beta \ln t \quad (6)$$

The slope and intercept of plot of q_t vs. ln t were used to calculate the values of the constants 'a' and 'b' as shown in (Fig. 5a.) and the constants are tabulated in Table 2.

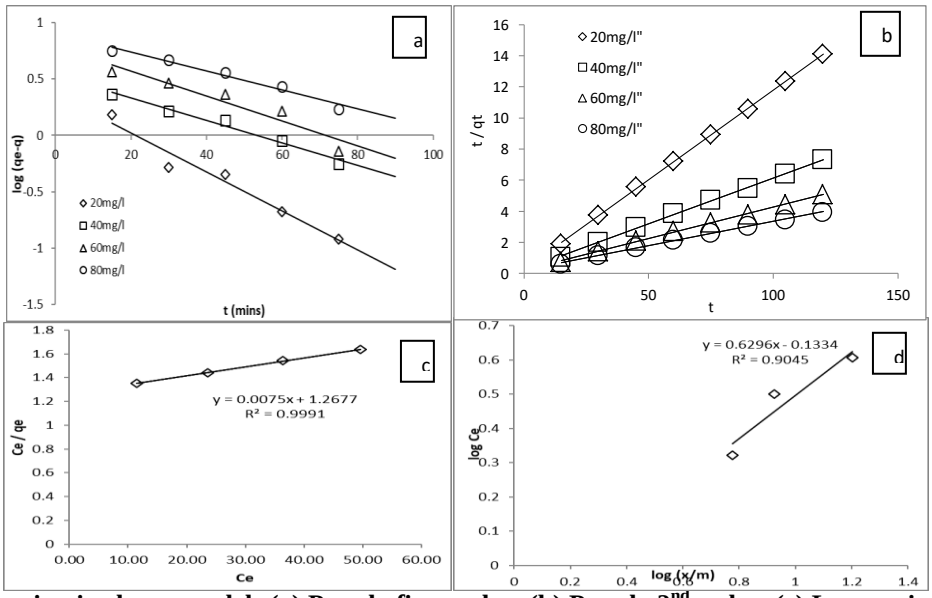

Fig.4. Adsorption isotherm models (a) Pseudo first order; (b) Pseudo 2nd order; (c) Langmuir; (d) Freundlich

3.3.3.3. Fractional power model

The fractional power model is a modified form of the Freundlich equation and can be expressed as:

$$\ln q_t = \ln a + b \ln t \quad (7)$$

where q_t the amount of the dyes sorbed by the adsorbent at time't' and 'a' and 'b' are constants with b < 1. The function 'a' 'b' is also a constant, being the specific sorption rate at unit time, i.e., when t = 1. The plot of lnt vs lnqt showed the linear relationship and the computed

constants 'a' and 'b' from the intercepts and slopes of the plots are presented in Fig. 5b. Table 2].

Table .1. Pseudo first order, second order, Langmuir and Freundlich constants for Rhodamine B dye onto AC-SiO_2 nanocomposite

Conc (ppm)	Pseudo first order	Pseudo second order			Freundlich			Langmuir		
	K_{ad} (min^{-1})	K_2	h	R^2	R^2	K_f	n	Q_o	b	R^2
20	3.98	259.7451	3.447087	0.9997	0.9045	0.7355	1.5883	133.3	169	0.9991
40	2.30	1278.088	4.418913	0.9991	0.8936	0.4899	1.1291			
60	2.56	2657.642	4.359198	0.9986	0.9081	0.9741	1.3226			
80	1.93	4512.516	4.420866	0.9978	0.9177	1.7608	1.4605			

3.3.3.4. Harkin's–Jura adsorption isotherm.

This can be expressed as

$$1/q_e^2 = (B/A) - (1/A) \log C_e \quad (8)$$

Where B and A are the isotherm constants. The Harkins–Jura adsorption isotherm accounts to multilayer adsorption and can be explained with the existence of a heterogeneous pore distribution. $1/q_e^2$ was plotted Vs. log Ce [Fig.5c. Table 2.]

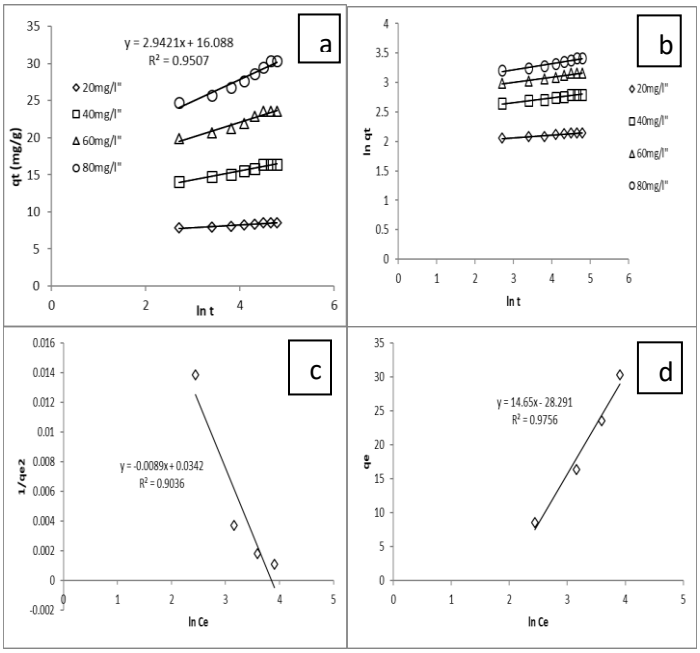

Fig.5. Adsorption isotherm models (a) Elovich (b) Fractional power model (c) Harkins-Jura (d) Tempkin isotherm

3.3.3.5. Tempkin model

The Tempkin isotherm equation is given as

$$q_e = RT/b \ln (KTC_e) \quad (9)$$

or

$$q_e = B \ln KT + B \ln C_e \quad (10)$$

where A = KT; B = RT/b, T is the absolute temperature in K, R is Universal gas constant, 8.314 J/mol/ K, KT the equilibrium binding constant (l/mg) and B is related to the heat of adsorption [29]. A plot of q_e vs ln C_e at studied temperature is given in Fig.5d. The constants obtained for Tempkin isotherm are shown in Table 2. The Tempkin constant B shows that the heat of adsorption decreases with the increase in temperature, indicating exothermic adsorption [30]. A uniform distribution of binding sites on the nanocomposite surface was also confirmed by the Tempkin isotherm.

Table.2. Elovich, Fractional power model, Harkins-Jura plot and Tempkin model constants for Rhodamine B adsorption onto AC-SiO_2 nanocomposite

Model	**Constants**			
Elovich	**Conc (ppm)**	**α**	**β**	**R^2**
	20	6.7886	0.3635	0.9403
	40	10.632	1.2149	0.9646
	60	14.124	1.9957	0.9434
	80	16.088	2.9421	0.9507
Fractional Power	**Conc (ppm)**	**a**	**b**	**R^2**
	20	6.897783	0.0444	0.9429
	40	11.25261	0.0796	0.9705
	60	15.29766	0.0916	0.9513
	80	18.10159	0.1079	0.9611
Harkin's Jura		**R^2**	**A**	**B**
		0.9991	133.333	169.027
Tempkin		**a**	**b**	**p**
		0.14498	14.65	170.2526

4. CONCLUSION

Synthesis of AC- SiO_2 nanocomposite sphere has been achieved by a simple and cost effective microwave assisted sol-gel method. The presence of AC in the SiO_2 has been revealed by SEM with EDX, -TEM, UV-Vis, XRD and FTIR analysis. The results confirmed the formation of AC-SiO_2. With an average particle size of 40 nm. The decrease in the particle size is related with the observed increase of the surface area. EDX and XRD reveal the presence of Si, O and C in the AC-SiO_2. TEM and SEM images reported nanocomposite spheres without aggregation. UV-vis showed the decrease in the direct band gap energy of the composite. The enhanced photocatalytic activity of AC-SiO_2 may be due to increased surface area, decreasing band gap energy and reduction in the recombination of electron-hole pairs along with increase of •OH radicals.

REFERENCE

[1] Kandula, S.; Jeevanandam, P.(2015): A facile synthetic approach for SiO_2@Co_3O_4 core–shell nanorattles with enhanced peroxidase-like activity. *RSC Adv.**5***, pp.5295–5306.

[2] Schaefer, C. G.; Vowinkel, S.; Hellmann, G. P.; Herdt, T.; Contiu, C.; Schneider, J. J.; Gallei.; M. A (2014): polymer based and template-directed approach towards functional multidimensional micro-structured organic/inorganic hybrid materials. *J. Mater. Chem., **2***, pp. 7960–7975.

[3] Yuliati, L.; Tsubota, M.; Satsuma, A.; Itoh, H.; Yoshida, H(2006): Photoactive sites on pure silica materials for nonoxidative direct methane coupling, *J. Catal*., ***238***, 214–220.

[4] Bal, R.; Tope, B. B.; Das, T. K.; Hegde, S. G.; Sivasanker, S. (2001): Alkali loaded silica, a solid base:investigation by FTIR spectroscopy of adsorbed CO_2 and its catalytic activity, *J. Catal*. ***204***, pp.358-363.

[5] Senthilvelan, S.; Chandraboss, V. L.; Karthikeyan, B.; Natanapatham, L.; Murugavelu, M.(2013):TiO_2, ZnO and nanobimetallic silica catalyzed Photodegradation of methyl green, *Mater. Sci. Semicond. Process.,**16***, pp.185–192.

[6] Chandraboss, V.L.; Senthilvelan, S.; Natanapatham, L.; Murugavelu, M.; Loganathan, B.; Karthikeyan, B.(2013): Photocatalytic effect of Ag and Ag/Pt doped silicate non crystalline material on methyl violet -Experimental and theoretical studies. *J. Non-Cryst. Solids, **368,*** pp. 23–28.

[7] Loganathan, B.; Chandraboss, V.L.; Murugavelu, M.; Senthilvelan, S.; Karthikeyan,B.(2015): Synthesis and characterization of multimetallic-core and siliceousshell Au/Pt/Ag@SiO2 sol– gel derived nanocomposite., *J. Sol-Gel Sci. Technol*., ***74***, pp. 1-14.

[8] Da Silva, L. M. L.; Da C. Silva, F.; De Carvalho, A. L.; Marcal, L.; Saltarelli, M.; De Faria, E. H.; Rocha, L. A.; Calefi, P. S.; Ciuffi, K. J.; Nassar, E. J.(2012): Influence of the Percentage of TiO_2 doped into SiO_2 Matrix on Photocatalysis, *ISRN Nanomater*., DOI:10.5402/2012/304546.

[9] Stober, W.; Fink, A.; Bohm, E.(1968): Controlled growth of mono disperse silica spheres in the micron size range, *J. Colloid Interface Sci*., ***26***, pp.62–69.

[10] Andriantsiferana, C.; Mohamed E. F.; Delmas, H.(2013): Photocatalytic degradation of an azo-dye on TiO_2/activated carbon composite material, *Environ. Technol*. 2013, DOI:10.1080/09593330.2013.828094.

[11] Pozzo, R. L.; Baltan, M. A.; Cassano, A. E. (1997): Supported titanium oxide as photocatalyst in water decontamination: state of the art. *Catal Today*.,***39***, pp.219–231.

[12] Chandraboss, V. L.; Kamalakkannan, J.; Prabha, S.; Senthilvelan, S.(2015): An efficient removal of methyl violet from aqueous solution by an AC-Bi/ZnO nanocomposite material, *RSC Adv*., ***5***,pp. 25857–25869..

[13] Tsumura, T.; Kojitani, N.; Umemura, H.; Toyoda, M.; Inagaki, M. (2002):Composites between photoactive anatase- type TiO_2 and adsorptive carbon. *Appl Surf Sci*.,***196***, pp. 429–436.

[14] Velasco, L. F.; Parra, J. B.; Ania, C. O.(2010): Role of activated carbon features on the photocatalytic degradation of phenol, *Appl. Surf. Sci*.,***256***, pp.5254–5258.

[15] Mezohegyi, G.; van der Zee, F. P.; Font, J.; Fortuny, A.; Fabregat, A.(2012): Towards advanced aqueous dye removal processes: A short review on the versatile role of activated carbon, *J. Environ. Manage*,***102***, pp. 148-164.

[16] Selhan Karago¨z,, Turgay Tay , Suat Ucar , Murat Erdem.(2008):Activated carbons from waste biomass by sulfuric acidactivation and their use on methylene blue adsorption. Biores. Technol., **99,** pp. 6214–6222.

[17] Jinlong Li, Deshuai Zhen, Guozhe Sui, Chunming Zhang, Qigang Deng, and Lihua Jia.(2012):Nanocomposite of Cu–TiO2–SiO2with high photoactive performance for degradation of Rhodamine B dye in aqueous wastewater, Journal of Nanoscience and Nanotechnology,**12**, pp. 6265–6270.

[18] Mahesh, K.P.O.; Kuo, D.H.; Huang B.R.(2015): Facile synthesis of hetero structured Ag-deposited SiO_2@TiO_2 composite spheres with enhanced catalytic activity towards the photodegradation of AB1 dye, J. Mol. Catal. A: Chem. **396**, pp. 290-296.

[19] Wang, X.; Xi, M.; Wang, X.; Fong, H.; Zhu, Z.(2016): Flexible composite felt of electrospun TiO_2 and SiO_2 nanofibers infused with TiO_2 nanoparticles for lithium ion battery anode, Electrochim. Acta., **190,** pp. 811-816.

[20] Dariania,R.S.;Esmaeilia,A.;Mortezaalia,A.; Dehghanpour,S.(2016):Photocatalytic reaction and degradation of methylene blue on TiO_2 nano-sized particles. Optik, **127,** pp. 7143–7154

[21] Ling, C.; Mohamed, (2004): Photo degradation of methylene blue dye in aqueous stream, J. Technol. **40,** pp. 91–103.

[22] Ghorai, S.; Sarkar, A.; Raoufi, .;, Panda, A. B.; Schönherr, H.; Pal, S.(2014): *ACS app. mater. & interfaces*. **6,** pp. 4766-4777

[23] Hesham Fouad Aly, Ahmed Ibrahim Abd-Elhamid.(2018): Photocatalytic degradation of Methylene blue dye Using Silica oxide nanoparticles as a catalyst. Water Environment Research, **9**, pp. 807-818.

[24] Matthews, R.W.(1989): Photocatalytic oxidation and adsorption of Methylene blue on thin films of near – UV illuminated TiO_2 J. Chem. Soc. Fara. Trans., **85,** pp. 1291–302.

[25] Dongen Zhang, Jinbo Wu, Bingpu Zhou, Yaying Hong, Shunbo Lia and Weijia Wen. Efficient photocatalytic activity with carbon-doped SiO_2 nanoparticles, Nanoscale, DOI: 10.1039/c3nr01314f.

[26] Chaudhuri,H.; Dash, S.; Sarkar, A.(2016): Adsorption of different dyes from aqueous solution using Si-MCM-41 having very high surface area. J. Porous Mater., **23**(5), pp.1227-1237.

[27] Hazzaa,R.;Hussein, M.(2015): Adsorption of cationic dye from aqueous solution onto activated carbon Prepared from olive stones. Environ. Technol. Innovat., **4,** pp. 36-51.

[28] Ghaedi,M.; Ghaedi, A.M.; Hossainpour, M.; Ansari,A.; Habibi,M.H. Asghari,A.(2014): Least square-support vector (LS-SVM) method for modeling of Methylene blue dye adsorption using copper oxide added onactivated carbon: Kinetics and isotherm study Ind. Eng. Chem. Res. **20**(4), pp.1641-1649.

[29] Foo, K.Y. (2012): Preparation, characterization and evaluation of adsorptive properties of orange peel based activated carbon via microwave induced K_2CO_3 activation. Bioresour. Technol., 104, pp.679–686.

[30] Wang, X.S; Qin, Y.(2005): Equilibrium sorption isotherms for of Cu^{2+} on rice bran. Process Biochem., **40**, pp. 677–680.